Longitudinal quantification of the GCF proteome during progression from gingivitis to periodontitis in a canine model

Davis, Ian J; Jones, Andrew; Creese, Andrew; Staunton, Ruth; Atwal, Jujhar ; Chapple, Iain; Harris, Stephen ; Grant, Melissa

DOI:
10.1111/jcpe.12548

Document Version
Peer reviewed version

Citation for published version (Harvard):
Davis, IJ, Jones, A, Creese, A, Staunton, R, Atwal, J, Chapple, I, Harris, S & Grant, M 2016, 'Longitudinal quantification of the GCF proteome during progression from gingivitis to periodontitis in a canine model', Journal of Clinical Periodontology. https://doi.org/10.1111/jcpe.12548

Longitudinal quantification of the GCF proteome during progression from gingivitis to periodontitis in a canine model

Ian J. Davis[‡°], Andrew W. Jones[†°], Andrew J. Creese[†], Ruth Staunton[‡], Jujhar Atwal[‡], Iain L.C. Chapple[†], Stephen Harris[‡] and Melissa M. Grant[†*]

[†] Periodontal Research Group, School of Dentistry, College of Medical and Dental Sciences, University of Birmingham, St. Chad's Queensway, Birmingham, B4 6NN, United Kingdom

[‡] The WALTHAM Centre for Pet Nutrition, Waltham-on-the-Wolds, Melton Mowbray, Leicestershire, LE14 4RS, United Kingdom

Running title: GCF proteome from gingivitis to periodontitis

* Address correspondence to: Melissa M. Grant, School of Dentistry, University of Birmingham, St. Chad's Queensway, Birmingham, B4 6NN, UK. Telephone: +44 (0)121 466 5520. Email: m.m.grant@bham.ac.uk

°These authors contributed equally

Keywords

Dog, periodontitis, gingivitis, proteomics, longitudinal, inflammation

Conflict of Interest and Sources of Funding

This work was funded by Mars Petcare the employer of the authors at the WALTHAM Centre for Pet Nutrition. Together with the University of Birmingham the WALTHAM Centre for Pet Nutrition was involved in the experimental design, sample collection, data collection, data analysis and preparation of the manuscript. The Advion TriVersa NanoMate, Dionex LC and Thermo Fisher Scientific Orbitrap Velos mass spectrometer used in this research were funded through the Birmingham Science City Translational Medicine: Experimental Medicine Network of Excellence project, with support from Advantage West Midlands (AWM).

Clinical Relevance: Changes in the GCF biotype during the transition from gingivitis to periodontitis are of diagnostic interest. As human studies are precluded due to the length of study this work offers a unique opportunity to shed light on proteomic changes during periodontitis and identify diagnostic biomarkers.

Principal Findings: Using state-of-the-art mass spectrometry we were able to identify significant increases in 40 proteins by mass spectrometry between mild periodontitis and gingivitis, and confirmed one protein by ELISA.

Practical Implications: The work shows that this approach is viable for the identification of biomarkers of periodontitis in GCF that change significantly during the transition from gingivitis to periodontitis in dogs. Further studies involving greater GCF volumes may help validate more biomarkers..

Acknowledgements

The authors thank Mark Marshall and Prof. Helen Cooper for their technical assistance and scientific input.

Abstract

Aim: Inflammatory periodontal disease is widespread in dogs. This study evaluated site-specific changes in the canine gingival crevicular fluid (GCF) proteome during longitudinal progression from very mild gingivitis to mild periodontitis. Periodontitis diagnosis in dogs requires general anaesthesia with associated risks and costs; our ultimate aim was to develop a periodontitis diagnostic for application in conscious dogs. The objective of this work was to identify potential biomarkers of periodontal disease progression in dogs.

Materials and methods: GCF was sampled from a total of ten teeth in eight dogs at three different stages of health/disease and samples prepared for quantitative mass spectrometry (data available via ProteomeXchange; identifier PXD003337). A univariate mixed model analysis determined significantly altered proteins between health states and six were evaluated by ELISA.

Results: 406 proteins were identified with 84 present in all samples. The prevalence of 40 proteins was found to be significantly changed in periodontitis relative to gingivitis. ELISA measurements confirmed that haptoglobin was significantly increased.

Conclusions: This study demonstrates for the first time that proteins detected by mass spectrometry have potential to identify novel biomarkers for canine periodontal disease. Further work is required to validate additional biomarkers for a periodontitis diagnostic.

Introduction

Periodontitis is the most widespread oral disease in dogs; depending on the population studied between 44% and 64% of dogs are affected (Butkovic et al., 2001; Kyllar et al., 2005; Kortegaard et al., 2008; Hamp et al., 1984). Variations in prevalence estimates are likely due to the different age and breed compositions of the study groups and the diagnostic criteria employed to define periodontitis. In humans the prevalence is estimated at 47% in adults over 30 years and over 70% in adults older than 65years (Eke et al 2012), highlighting the variation with age in a divergent mammal.

It is widely accepted that dysbiosis within the human dental plaque biofilm is the primary initiator of periodontitis (Roberts & Darveau 2015); though how these organisms trigger disease and the basis for the subsequent pathological events thereafter appears to be host-mediated (Bartold & VanDyke 2013). One working hypothesis is that specific antigens or enzymes produced by bacteria within the plaque biofilm initiate the activation of the host inflammatory response, which fails to resolve and becomes chronic and destructive in nature (VanDyke 2009). The dog oral microbiome was recently investigated by Dewhirst et al (2012). The study demonstrated that these divergent mammalian species (dog versus human) only share 16.4% of oral taxa when the accepted 98.5% 16S rRNA sequence similarity cut off was employed. However, studies over the last 40 years have demonstrated that plaque is also the initiating factor of periodontal inflammation in dogs (Egelberg 1965; Lindhe et al 1975). From a 16S rRNA pyrosequencing study of plaque in a cross-sectional cohort study of dogs we identified a number of bacterial species whose prevalence was associated with either health or early periodontitis (Davis et al 2013). More recently we followed 52 miniature schnauzers, a small-sized breed at risk of developing periodontitis, for 60 weeks (Marshall et al 2014) without any tooth cleaning regimes. Thirty five of these animals had 12 or more teeth develop periodontitis during the course of the study and the incisors were the most likely to develop disease on the lingual aspect. Older dogs developed periodontitis more rapidly than younger dogs. This study illustrated the speed with which periodontitis can develop in a small breed of dog in the absence of any oral hygiene regime.

In both humans and dogs the initial stages of periodontal disease are observed clinically as red and inflamed gingivae, defined as “gingivitis”. Without treatment to remove and disrupt the plaque biofilm, gingivitis may progress to periodontitis. In dogs a periodontal scoring system based on levels of inflammation and probing periodontal pocket depths has been developed for diagnosis (Wiggs & Lopbrise, 1997). In this system periodontitis (PD) scoring is staged as absolute health (G0), through four levels of gingivitis increasing by severity (G1-G4) followed by four PD levels (PD1-PD4) with PD4

being the most severe and PD1 being very early periodontitis. To accurately assess the periodontal health of a dog, specialist veterinary dental expertise, periodontal probing pocket depths and radiological confirmation under general anaesthesia are required. As this expertise is not always available in an average clinical setting and to reduce the anaesthetic burden of pets the current program of work set out to identify protein biomarkers for periodontitis in dogs. The ultimate aim being to develop a diagnostic tool that may be used to screen GCF or saliva taken from conscious dogs. A mass spectrometry based proteomics approach was applied to a naturally occurring longitudinal periodontitis sample set.. The sample archive studied was unique in that it was collected from a longitudinal study of disease progression. The samples were selected from 52 miniature schnauzers as they progressed from health to mild periodontitis over a 60-week period prior to scaling and prophylaxis to arrest disease progression and re-establish health (Marshall et al., 2014).

For the non-presumptive analysis of proteins detected in oral fluids, mass spectrometry based proteomics is acknowledged as the best tool available; hence it was selected for this study (Grant 2012). The technology confers the ability to examine the complex composition of oral fluids, such as gingival crevicular fluid (GCF) and saliva which can facilitate the identification of biomarkers of health and disease. Advances in recent years mean that proteins can be compared quantitatively across samples by the addition of isobaric mass tags (e.g. ITRAQ or TMT labels) (Grant et al 2010) or by label free quantitation (Bostanci et al 2010 & 2013) in these fluids. So far human studies of experimental gingivitis (Grant et al 2010 and Bostanci et al 2013) or of periodontitis (Bostanci et al 2010; Trinidade et al 2015) have yielded large number of proteins, allowing for an in-depth insight into inflammatory diseases of the gingivae. However to date it has not been possible to follow human participants during the progression from health to gingivitis and subsequently to periodontitis in the same individuals. The challenges to complete such an investigation include extended timescales, the significant resource to screen volunteers regularly enough to meet ethical considerations and the subsequent impact on volunteer retention and expense.

Methods

Longitudinal Trial Design and Scoring Criteria

In a previous longitudinal study individual teeth were tracked in 52 dogs (equating to 2155 teeth) with dental assessments under general anaesthesia at 6 weekly periods up to 60 weeks. The disease stage of each tooth was assessed using the Wiggs & Lopbrise PD scoring system described in full by Marshall et al (Wiggs & Lopbrise, 1997; Marshall et al., 2014) and shown for the stages used in the present study in table 1. Probing pocket depth was measured from the gingival margin to the bottom of the periodontal pocket. Gingival recession was measured from the cementoenamel junction (CEJ) to the gingival margin. Total attachment loss was calculated as the sum of the gingival recession and the periodontal probing pocket depth in accordance with established protocols (Harvey 2005). Samples of gingival crevicular fluid and subgingival plaque were taken and archived at each time point (Marshall et al., 2014). In this way very mild gingivitis (G1) and moderate gingivitis (G3) samples were collected from all teeth that eventually progressed to mild periodontitis (PD1). A subset of these samples from 10 teeth in 8 dogs was used in the present study. The mean age of the dogs sampled was 3.2 years (SE $\pm$ 0.5) and genders were equally balanced (Table 2). The study was approved by the WALTHAM® Animal Welfare and Ethical Review Body and run under licensed authority in accordance with the UK Animals (Scientific Procedures) Act 1986. At the end of the study all dogs had prophylactic treatment including a scale and polish and tooth brushing to re-establish healthy gingiva.

All teeth were scored individually based upon a modified Wiggs & Lobprise scoring system described in full by Marshall *et al*. (2014). In short: a gingivitis score between 0 and 4 was recorded for the mesial, mid-buccal, distal and palatal/lingual aspect of each tooth using a modified combination of the gingival index (GI) and sulcus bleeding index (SBI). Periodontitis stage 1 (PD1) was classified as being up to 25% attachment loss. Probing depths were measured from the gingival margin to the base of the periodontal pocket.

Collection and Preparation of Clinical Samples

Gingival crevicular fluid (GCF) samples were collected on paper points for 30 seconds and stored at -80 °C. Samples included in the study were selected in order to represent a variety of tooth types from a number of different dogs as the teeth progressed from very mild (G1) to moderate (G3) gingivitis through to mild periodontitis (PD1). A total of ten teeth at three time points (representing each health state) from a total of eight miniature schnauzers (30 samples in total) were chosen (Table 2). Proteins were extracted from the paper points by wetting with ammonium bicarbonate buffer (100 mM, 400 µl), vortexing for 30 s and the solution was then placed into a clean snap top

Eppendorf tube. Further ammonium bicarbonate (100 mM, 200 µl) was added to the GCF containing paper points to remove any retained proteins, vortexed for 30 s, centrifuged at 13,000 r min^{-1} for 5 min, and added into the initial extraction solution resulting in a single fluid containing tube (600 µl). Dithiothrietol (50 mM, 20 µl) was added to the samples and incubated at 60 °C for 45 min. The samples were returned to room temperature, prior to addition of iodoacetamide (22 mM, 100 µl) and incubated at room temperature in the dark for 25 min. A further small volume of dithiothrietol (50 mM, 2.8 µl) was added to quench any unreacted iodoacetamide. Trypsin (0.4 µg) was added to each sample and incubated overnight at 37 °C. The samples were vacuum centrifuged dry, resuspended in trifluoroacetic acid (TFA) (200 µl, 0.5 % v/v), de-salted using a C_{18} MacroTrap (Michrom, Auburn, CA, USA) and again vacuum centrifuged dry.

For comparison a small equivalent fraction from all GCF samples was pooled (master sample mix) and labelled with an iTRAQ mass tag of 117. Very mild gingivitis (G1), moderate gingivitis (G3) and mild periodontitis (PD1) samples were labelled with iTRAQ (4plex, AB SCIEX) labels 114, 115 and 116, respectively. All samples were incubated with the labels for two hours before being pooled into individual tooth samples.

The ten combined samples (containing 3 samples per tooth, one at each stage of health or disease) were vacuum centrifuged dry and resuspended in mobile phase A (10 mM KH_2PO_4, 20 % (v/v) acetonitrile, pH 3, 100 µl) for strong cation exchange (SCX) liquid chromatography. The peptides were separated on a polysulfethyl A column (100 mm × 2.1 mm, 5 µm particle size, 200 Å pore size; PolyLC, Columbia, MD, USA) with a javelin guard cartridge (10 mm × 2.1 mm, 5 µm particle size, 200 Å pore size; PolyLC) using mobile phase A and mobile phase B (10 mM KH_2PO_4, 500 mM KCl, 20 % (v/v) acetonitrile, pH 3). The separation gradient ran 0 to 80% mobile phase B over 90 min, resulting in 17 × 750 µl fractions. Fractions 1-4, 5-7, 8-10, and 11-17 were combined to provide four fractions. Each fraction was vacuum centrifuged to ~50 µl and desalted using C_{18} ZipTips (Millipore). The desalted peptides were vacuum centrifuged dry and resuspended in formic acid (20 µl, 0.1 (v/v)).

Mass Spectrometry

Online LC-MS/MS was performed on a Dionex UltiMate 3000 RLSCnano (Thermo Fisher Scientific, Bremen, Germany) system coupled to an LTQ-Orbitrap Velos ETD (Thermo Fisher Scientific). Peptides were loaded onto a 150 mm Acclaim PepMap100 C_{18} column (LC Packings, Sunnyvale, CA, USA) in formic acid (0.1 % (v/v)), and separated over a 90 min linear gradient from 3.2 % to 44 % mobile phase B (acetonitrile with formic acid (0.1 % (v/v)) with a flow rate of 350 nl min^{-1}. The column was

then washed with 90 % mobile phase B before re-equilibrating at 3.2 % mobile phase B. The column was maintained at 35 °C. The LC system was coupled to an Advion Biosciences TriVersa NanoMate source (Ithaca, NY, USA) which infused the peptides with a spray voltage of 1.7 kV. Peptides were infused directly into the mass spectrometer. The mass spectrometer performed a full FT-MS scan (*m/z* 380-1,600) and subsequent collision induced dissociation (CID, 35% normalized collision energy NCE) MS/MS scans of the three most abundant ions followed by higher energy collisional dissociation (HCD 55 NCE) of the same three ions. Analysed ions were placed on an exclusion list for 60 s. The CID and HCD spectra were used for peptide identification and quantification, respectively. Each SCX set (*i.e.* the four SCX fractions from each sample) was run in sequence followed by a blank and repeated in triplicate.

Mass Spectrometry Data Processing and Annotation

The data were analysed using Proteome Discoverer (version 1.4, Thermo Scientific). Data from each SCX set were analysed together and each replicate searched independently. Mascot and SEQUEST algorithms were used to search the data with identical settings used. The database was the UniProt *Canis lupus familiarus* (29,293 entrants downloaded 02/2014). The data were searched with the following settings: trypsin as the enzyme with a maximum of two missed cleavages, 10 ppm mass accuracy for the precursor ion, fragment ion mass tolerance was set at 0.8 Da, carbamidomethylation of cysteine and iTRAQ addition to the N-terminus and lysine residues were set as fixed modifications, and phosphorylation of serine, threonine and tyrosine was set as a variable modification as was oxidation of methionine and iTRAQ addition to tyrosine. The search results from each of the technical replicates were combined and proteins which were identified with two or more unique peptides were classed as identified. Only unique peptides were used for protein quantification (performed in Proteome Discoverer) and protein grouping was employed (only proteins which contained unique peptides were used). The mass spectrometry proteomics data have been deposited to the ProteomeXchange Consortium (Vizcaíno et al 2014) via the PRIDE partner repository with the dataset identifier PXD003337.

ELISA Methodology

In an attempt to corroborate the Mass spectrometry findings, samples were screened on canine specific assays for Pyruvate kinase (TSZELISA,USA; limit of detection 1.56ng/ml), Haptoglobin (Life Diagnostics Incorporated, USA; limit of detection 1.95ng/ml), Calcium binding protein S100A8 (NeoBioLab, USA; limit of detection 156.25pg/ml), Myosin 9 (Wuhan EIAab Science Co. Ltd, China; limit of detection 31.2pg/ml), Type 1 dog keratin cytoskeletal 10 (Wuhan EIAab Science Co. Ltd,

China; limit of detection 0.31ng/ml) and Canine anti-immunoglobulin binding protein (MyBioSource,USA; limit of detection 0.3125μg/ml).

Due to the limited amount of protein in each GCF sample it was not possible to screen each tooth sample against the six different ELISAs; hence a G1 and PD1 sample from the same tooth was screened with a single ELISA. Samples from ten dogs were screened on each ELISA (see supplementary data table 2 for the 60 teeth screened). The samples were selected from the biobanked samples from the wider study (Marshall et al 2014) from teeth with the most similar characteristics in terms of progression from G1 to PD1 and location to those used in the proteomics discovery experiments. GCF paper point samples were suspended in sterile phosphate buffered saline (PBS) with volumes varying dependent on the manufacturer's instructions, typically between 110 and 210μl. The sample was thoroughly mixed and centrifuged, paper points were then trapped in the lid of the tubes and centrifuged again for complete elution. The eluted sample was assayed in duplicate immediately according to the manufacturer's instructions. The assays were quantitative solid phase sandwich enzyme linked immunoassays with the exception of the Calcium binding protein S100A8 and Type 1 dog keratin cytoskeletal 10 which were competitive binding immunoassays.

Statistical Analysis

An analysis was performed to determine which mass spectrometry proteins were observed in samples at significantly different levels between health states. To prioritise proteins that would be relevant as biomarkers only proteins identified in at least one replicate in all 10 teeth, regardless of health state, were included in this analysis. The $\log_e$ transformed abundance of each protein was analysed univariately using mixed effects methodology with health state as the fixed effect and health state nested in tooth as the random structure. For each protein, abundances for each health state and fold changes between health states were estimated with 95% confidence intervals. Due to the increased risk of false positives with the analysis of many proteins, *p*-values were adjusted using the Benjamini-Hochberg false discovery rate method (Benjamini & Hochberg, 1995). Putative functions were curated from the Uniprot entry for each protein.

For statistical analysis of the ELISA data, the $\log_e$ transformed protein concentration was analysed using a mixed effects model with health state as the fixed effect and tooth as the random effect. The concentration for each health state and fold changes between health states were estimated with 95% confidence intervals.

All statistical analyses were performed in R version 3.2.0 (2015-04-16), The R Foundation for Statistical Computing (www.r-project.org). Packages used were lme4 (Bates et al 2014) and multcomp (Hothorn et al 2008).

Results

Proteomic analysis of GCF samples

GCF samples collected from ten teeth at three time points from a total of eight miniature schnauzers (30 samples in total) were included in the study. The samples represented periodontal disease progression from very mild (G1) to moderate (G3) gingivitis through to mild periodontitis (PD1). Table 2 illustrates the time taken for the development to each stage for each tooth. The mean (+/- SE) for progression between states was: G1 to G3 15.6 (± 2.4) weeks; G3 to PD1 14.4 (± 2.8) weeks; and G1 to PD1 30.0 (± 4.1) weeks.

Cumulatively, a total of 406 canine proteins were identified and quantified, after passing the 1% peptide false discovery rate, in at least one LC-MS/MS run. Variations between teeth in the prevalence of these proteins at each disease state are shown in figure 1. This hive panel demonstrates the intra-individual variation between samples, depicting both changes per tooth type and within an individual subject. Neither the rate of progression nor the putative size of the tooth appeared to be correlated with the quantity of proteins at each stage when examining individual teeth. Indeed where the same dog developed inflammation in two teeth across the course of the study the two teeth showed remarkably individual responses.

Of the 406 proteins, 84 (20.7%) were identified in at least one triplicate run for all ten GCF samples (Supplemental Table 1). The quantified values of the 84 proteins found in all samples are represented in Figures 2 showing the variation in protein intensity between very mild gingivitis, moderate gingivitis, and periodontitis. Figure 3 shows the fold changes in proteins between moderate gingivitis: very mild gingivitis (G3/G1), mild periodontitis: very mild gingivitis (PD1/G1) and mild periodontitis: moderate gingivitis (PD1/G3). It is interesting to note that there appears to be a much greater increase in total protein amount in mild periodontitis in comparison to both stages of gingivitis (figure 2); whereas both moderate gingivitis vs very mild gingivitis and mild periodontitis vs very mild gingivitis have large variations (figure 3). This could be explained if greater GCF volumes were obtained from periodontitis sites than healthy or gingivitis sites; however a limitation of the present study was that we did not measure GCF volumes obtained. As a consequence of the greater increase in protein in mild periodontitis separation between disease, *i.e.* mild periodontitis or moderate gingivitis, and very mild gingivitis is easily identified, whereas identification between mild periodontitis and moderate gingivitis is far more difficult.

To investigate which proteins changed significantly between disease states, a univariate mixed model analysis of these proteins was employed. Eighty-four proteins were identified as being present in at least one replicate in all 10 teeth, resulting in 252 comparisons between the three health states. Of these, 58 contrasts from 40 different proteins were significant after Benjamini-Hochberg correction (Table 3). These significant differences in protein prevalence were either between very mild gingivitis (G1) and PD1 or moderate gingivitis (G3) and PD1. No significant differences were observed in protein prevalence between very mild and moderate gingivitis. All proteins with significant changes increased in prevalence through the disease process with the greatest fold changes observed in haptoglobin, S100A8, haemoglobin subunit beta, S100A12, Fibrinogen beta chain and 14-3-3 protein beta/alpha. Eight of the significant proteins were uncharacterised; the remaining proteins could be grouped by function as relevant to immunity and inflammation, blood constituents, structural, metabolic, housekeeping and biosynthetic by gene ontology analysis.

ELISA verification of proteomic analysis

Of the six proteins screened by ELISA, only haptoglobin was detected in all GCF samples tested. A significant difference in haptoglobin concentration was observed between the health states (p=0.0001) with a 2.17 fold change between PD1/G1 (95% CI = 1.46, 3.22) by ELISA compared to the estimated 2.48 fold change (95% CI = 1.32, 4.66) from the mass spectrometry results (figure 4 & table 3). PBS adversely altered the sensitivity of both S100A8 and immunoglobulin binding protein assays and detection for these proteins in GCF samples was not conclusive. Myosin 9 and Keratin type 1 cytoskeletal 10 proteins could be detected at low levels in some GCF samples but several samples were below the limit of detection (supplementary data table 2) limiting conclusions to be drawn. Pyruvate Kinase could not be detected in any samples.

Discussion

The present study has investigated for the first time site specific longitudinal changes in the GCF proteome quantitatively from miniature Schnauzers that naturally develop periodontitis. With our experimental design we were able to follow eight individuals and ten teeth across the course of the 60 week study. This yielded data not only on inter-individual variation but also on intra-individual variation. Although this inter-individual variation was quite high it was possible to gain information on 84 proteins that were found in all samples. This was approximately 21% of the total proteins detected. The method employed, fragmentation and quantitation of the top three peptides in each duty cycle, will have significantly contributed to the variation observed. Other techniques such as MS^E (Levin et al 2011) and SWATH methods (Sajic et al 2015) could be employed in the future to gain more information with less missing data. Previously we have used pooled samples (Grant et al 2010), which will aid in more consistent protein identification but loses information on individual variation.

In this study we searched the mass spectrometry data against the open access reference dog database in Uniprot. However, by using an in-house database of microbial species detected by Dewhirst et al (2012) it was also possible to search against a combined database containing bacterial genome sequences from dog oral microbiota and dog proteomes. Although we are not presenting these data here, as the canine oral microbiota genome database has not been published, we only detected 28% bacterial proteins in the total number of proteins found. None of these bacterial proteins were detected in samples from all teeth. This is in agreement with other studies (Grant et al 2010, Bostanci et al 2010) as this type of metaproteomics is acknowledged to be associated with a number of problems. Indeed Kuboniwa et al (2012) highlighted that any system in which hundreds of individual species are present, such as in oral plaque, the proteins detected by proteomics will be dominated by a small number of peptides that are amenable to the approach used and that as the community complexity increases this effect becomes more pronounced. In communities with several highly related species, such as the *Streptococci*, it also becomes difficult to assign peptides to one species as the proteins may be highly homologous in sequence identity (Muth et al 2015). Additionally, traditional false discovery rate calculations breakdown, causing very conservative identifications of a few proteins or a larger number of identifications with less precision in identification (Muth et al 2015).

Through univariate analysis, 40 proteins were identified to be significantly increased between mild periodontitis and moderate gingivitis or mild periodontitis and very mild gingivitis. That no proteins were observed to increase significantly between very mild to moderate gingivitis may be due the size of the sample set limiting statistical power. The 40 significant proteins can be grouped

according to their function with structural proteins being most represented followed by those involved in immunity and inflammation. Within the structural group, keratins (5/11) make up nearly half of the proteins identified and they displayed very similar changes in profile across the study. Keratins indicative of both stratified and simple epithelia were found suggesting that there is destruction of both the sulcular and junctional epithelia occurring. Lymphocyte cytosolic protein 1 (LCP-1 or Plastin-2) is also classed as a structural protein and has been found in a number of proteomic studies examining GCF and saliva (Grant et al 2010, Bostanci et al 2010, Bostanci et al 2013). Öztürk et al (2014) have shown that it is a potential biomarker for periodontal diseases in humans. Additionally, there are a number of other proteins that are of likely neutrophilic in origin: the S100 proteins A8, 9 and 12, myeloperoxidase, neutrophil elastase and lysozyme. Neutrophils are the most abundant cells in the circulation and are found abundantly in human periodontal lesions (Scott & Krauss 2012). They are the first responding cells to infection and injury utilizing their protein and chemical arsenal to counteract the insult. For example, myeloperoxidase will produce hypochlorous acid, a strong bactericidal agent, and trigger for neutrophil extracellular trap release (Palmer et al 2012) and neutrophil elastase will degrade the extracellular matrix to allow neutrophil access to the site of action. The S100 proteins are a family of calcium binding proteins with multiple functions (Gross et al 2014). All three found here are abundant in neutrophils and S100A8 and S100A12 are known to be chemoattractive to neutrophils and will amplify neutrophil recruitment. S100A8 can be oxidised by reactive oxygen species produced by neutrophils and is rendered no longer a chemoattractant (Goyette & Geczy 2011). S100A12 however will still maintain the recruitment of neutrophils as it does not contain any oxidatively modifiable cysteine residues (Goyette & Geczy 2011). The presence of neutrophils will increase the amount of oxidative stress due to the production of reactive oxygen species. It is interesting to see the significant increase in two antioxidant response proteins, namely NQO1 and thioredoxin, across the course of the study. The redox balance between antioxidants and oxidants is important for prevention of bystander tissue damage (Chapple & Matthews 2007).

HSPA5 was found to be significantly increased in mild periodontitis compared to very mild gingivitis. One of the key functions of this protein in humans is in the unfolded protein response and endoplasmic reticulum (ER) stress (Baird et al 2013). Kebschull et al (2014) reported in a transcriptomic analysis of human gingival biopsies that ER stress related pathways were increased in periodontitis. Indeed, Baird et al (2013) demonstrated increases in HSPA5 in *ex vivo* cultured gastric cells infected with *Helicobacter pylori*. There is an acknowledged cross over in signalling pathways

between the innate immune and ER stress response pathways (Claudio et al 2013) and although this is just one protein, it may be an insight into how human and dog periodontal diseases overlap.

Overall the proteins found depict an inflammatory response with associated tissue destruction from neutrophils and the epithelium. These two cell types will be the most abundant adjacent to the GCF collection site and thus could be expected to contribute the most. This study used a top 3 technique for identification of peptides in the mass spectrometer. Greater depth and improved consistency, as mentioned above, may yield deeper insights and proteins from different origins. Complementary techniques such as multiplexed analysis of low abundance cytokines and chemokines could improve our understanding of the periodontal process in dogs. The results of the haptoglobin ELISA screen are proof of principle that the iTRAQ approach to discover biomarkers is sound. However the fact that only one in six of the canine ELISA kits were successful in quantifying protein in GCF samples presents a significant hurdle in validating these putative biomarkers. Whilst all of the ELISAs claim to be dog specific the main challenge appears to be one of sensitivity with the detectable concentration of target proteins in the GCF samples being so low. It is not clear if this is an issue with the specificity/ sensitivity of the ELISAs, relatively low levels of the proteins in GCF, degradation of the proteins whilst in storage or a combination of these. This challenge will need to be addressed if a canine GCF based periodontal disease diagnostic is to be developed. Further mass spectral techniques, which are independent of antibody specificities, such as selected or multiple reaction monitoring (SRM or MRM) are promising candidates (Harlan & Zhang 2014). Further verification or production of ELISAs aimed at detecting dog proteins is another, though, longterm option. For instance production of recombinant dog proteins to verify antibody specificity and analysis of post translational modifications may be important in this context. This is particularly relevant as a small panel of biomarkers will most likely the best way forward for robust detection of periodontal disease. Additionally, here we used GCF samples, rather saliva. As GCF requires technical expertise to collect it will also be important to validate biomarkers in saliva in the future.

A great advantage of our study is the possibility of examining the progression of very mild gingivitis to mild periodontitis. The current consensus statement views gingivitis and periodontitis as a continuum of chronic inflammatory disease (Tonetti et al 2015) in humans. However it is extremely difficult to assess the natural directional progression from gingivitis to periodontitis in humans. Therefore, our study represents a unique opportunity to examine natural progression in a canine model. The insights gained here not only could give rise to a tool to assist veterinarians but can also

shed light on progression of a disease common in the animal kingdom (Oz & Puleo et al 2011; Ismaiel et al 1989).

References

Baird, M., Woon Ang, P., Clark, I., Bishop, D., Oshima, M., Cook, M.C., Hemmings, C., Takeishi, S., Worthley, D., Boussioutas, A., Wang, T.C. & Taupin, D. (2013) The unfolded protein response is activated in Helicobacter-induced gastric carcinogenesis in a non-cell autonomous manner. *Laboratory Investigation* **93**:112-22. doi: 10.1038/labinvest.2012.131.

Bartold, P.M. & VanDyke, T.M. (2013) Periodontitis: a host-mediated disruption of microbial homeostasis. Unlearning learned concepts. *Periodontology 2000* **62**, 203–217.

Bates, D., Maechler, M., Bolker, B. & Walker, S. (2014). Fitting Linear Mixed-Effects Models using lme4., *Journal of Statistical Software*, arXiv:1406.5823v1

Benjamini, Y., & Hochberg, Y. (1995). Controlling the false discovery rate: a practical and powerful approach to multiple testing. *Journal of the Royal Statistical Society Series B*, **57**, 289–300. doi:10.2307/2346101

Bostanci, N., Heywood, W., Mills, K., Parkar, M., Nibali, L. & Donos, N. (2010) Application of label-free absolute quantitative proteomics in human gingival crevicular fluid by LC/MS E (gingival exudatome). *Journal of Proteome Research*. **9**:2191-9. doi: 10.1021/pr900941z.

Bostanci, N., Ramberg, P., Wahlander, Å., Grossman, J., Jönsson, D., Barnes, V.M. &, Papapanou, P.N. (2013) Label-free quantitative proteomics reveals differentially regulated proteins in experimental gingivitis. *Journal of Proteome Research*. **12**:657-78. doi: 10.1021/pr300761e.

Butkovic, V., Šimpraga, M., Šehic, M., Stanin, D., Sušic, V., Capaz, P. & Kos, J. (2001) Dental diseases of dogs: A retrospective study of radiological data. *Acta Veterinaria Brno* **70**: 203-208.

Chapple, I.L.C & Matthews, J.B. (2007) The role of reactive oxygen and antioxidant species in periodontal tissue destruction. *Periodontology 2000*. **43**:160-232

Claudio, N., Dalet, A., Gatti, E. & Pierre P (2013). Mapping the crossroads of immune activation and cellular stress response pathways. EMBO Journal 32:1214-1224. doi: 10.1038/emboj.2013.80.

Davis, I. J., Wallis, C., Deusch, O., Colyer, A., Milella, L., Loman, N. & Harris, S. (2013) A cross-sectional survey of bacterial species in plaque from client owned dogs with healthy gingiva, gingivitis or mild periodontitis. *PLoS ONE* **8**, e83158. doi:10.1371/journal.pone.0083158.

Dewhirst, F.E., Klein, E.A., Thompson, E.C., Blanton, J.M., Chen, T., Milella, L., Buckley, C.M., Davis, I.J., Bennett, M.L. & Marshall-Jones, Z.V. (2012) The canine oral microbiome *PLoS One*. **7**:e36067. doi: 10.1371/journal.pone.0036067.

Egelberg, J.(1965) Local effects of diet on plaque formation and gingivitis development in dogs. I Effect of hard and soft diets. *Odontologisk Revy*. **16**:31–41.;

Eke, P.I., Dye, B.A., Wei, L., Slade, G.D., Thornton-Evans, G.O., Borgnakke, W.S., Taylor, G.W., Page, R.C., Beck, J.D. & Genco, R.J. (2015) Update on Prevalence of Periodontitis in Adults in the United States: NHANES 2009 to 2012. *Journal of Periodontology*. **86**:611-22. doi: 10.1902/jop.2015.140520.

Goyette, J. & Geczy, C.L. (2011) Inflammation-associated S100 proteins: new mechanisms that regulate function. *Amino Acids* **41**:821–842. doi: 10.1007/s00726-010-0528-0.

Grant, M.M. (2012) What do 'omic technologies have to offer periodontal clinical practice in the future? *Journal of Clinical Periodontology* **47**:2-14. doi: 10.1111/j.1600-0765.2011.01387.x.

Grant, M.M., Creese, A.J., Barr, G., Ling, M.R., Scott, A.E., Matthews, J.B., Griffiths, H.R., Cooper, H.J., & Chapple, I.L.C. (2010) Proteomic Analysis of a Noninvasive Human Model of Acute Inflammation and Its Resolution: The Twenty-one Day Gingivitis Model. *Journal of Proteome Research* **9**: 4732–4744. doi: 10.1021/pr100446f.

Gross, S.R., Sin, C.G., Barraclough, R &, Rudland, P.S.(2014) Joining S100 proteins and migration: for better or for worse, in sickness and in health. *Cellular and Molecular Life Sciences*.**71**:1551-79. doi: 10.1007/s00018-013-1400-7.

Hamp, S.E., Ollon, S.E., Farso-Madsen, K., Viklands, P. & Fornell, D. (1984) A macroscopic and radiological investigation of dental diseases of the dog. *Veterinary Radiology* **25**: 86--92. doi: 10.1111/j.1740-8261.1984.tb01916.x

Harlan, R. & Zhang, H. (2014) Targeted proteomics: a bridge between discovery and validation. *Expert Reviews in Proteomics*. **11**:657-61. doi: 10.1586/14789450.2014.976558.

Harvey, C.E. (2005). Management of periodontal disease: understanding the options. *Veterinary Clinics of North America: Small Animal Practice* **35**: 819–836. doi: 10.1016/j.cvsm.2005.03.002

Hothorn, T., Bretz, F. & Westfall, P. (2008). Simultaneous Inference in General Parametric Models. *Biometrical Journal* **50**, 346-363. doi: 10.1002/bimj.200810425.

Ismaiel, M.O., JGreenman, J., Morgan, K., Glover, M.G., Rees, A.S., & Scully, C. (1989) Periodontitis in Sheep: A Model for Human Periodontal Disease. *Journal of Periodontology* **60**, 279-284

Kebschull, M., Demmer, R.T., Grün, B., Guarnieri, P., Pavlidis, P.& Papapanou, P.N. (2014) Gingival tissue transcriptomes identify distinct periodontitis phenotypes. *Journal of Dental Research* **93**:459-68. doi: 10.1177/0022034514527288.

Kortegaard, H.E., Eriksen, T &, Baelum, V. (2008) Periodontal disease in research beagle dogs - an epidemiological study. *Journal of Small Animal Practice* **49**: 610-616. doi: 10.1111/j.1748-5827.2008.00609.x.

Kuboniwa, M., Tribble, G.D., Hendrickson, E.L., Amano, A., Lamont, R.J. & Hackett, M. (2012) Insights into the virulence of oral biofilms: discoveries from proteomics. *Expert Reviews in Proteomics*. **9**:311-23. doi: 10.1586/epr.12.16.

Kyllar, M &, Witter, K. (2005) Prevalence of dental disorders in pet dogs. *Veterinarni Medicina* **50**: 496-505.

Levin, Y., Hradetzky, E. & Bahn, S. (2011) . Quantification of proteins using data-independent analysis (MSE) in simple and complex samples: a systematic evaluation. *Proteomics*. **11**:3273-87. doi: 10.1002/pmic.201000661.

Lindhe, J., Hamp, S.-E. & Loe, H. (1975) Plaque Induced periodontal disease in beagle dogs. A 4-year clinical, roentgenographical and histometrical study. *Journal of Periodontal Research*. **10**:243–255

Marshall, M. D., Wallis, C. V., Milella, L., Colyer, A., Tweedie, A. D. & Harris, S. (2014) A longitudinal assessment of periodontal disease in 52 Miniature Schnauzers. *BMC Veterinary Research* **10**: 166 doi: 10.1186/1746-6148-10-166.

Muth, T., Behne, A., Heyer, R., Kohrs, F., Benndorf, D., Hoffmann, M., Lehtevä, M., Reichl, U., Martens, L. & Rapp, E. (2015) The MetaProteomeAnalyzer: a powerful open-source software suite for metaproteomics data analysis and interpretation. *Journal of Proteome Research*. **14**:1557-65. doi: 10.1021/pr501246w.

Muth, T., Kolmeder, C.A., Salojärvi, J., Keskitalo, S., Varjosalo, M., Verdam, F.J., Rensen, S.S., Reichl, U., de Vos, W.M., Rapp, E. & Martens, L. (2015) Navigating through metaproteomics data: A logbook of database searching. *Proteomics*. doi: 10.1002/pmic.201400560.

Oz, H.S. & Puleo, D.A. (2011) Animal models for periodontal disease. *Journal of Biomedicine and Biotechnology*. 754857. doi: 10.1155/2011/754857.

Öztürk, V.Ö., Emingi,l G., Osterwalder, V. & Bostanci, N. (2015) The actin-bundling protein L-plastin: a novel local inflammatory marker associated with periodontitis. *Journal of Periodontal Research*. **50**:337-46. doi: 10.1111/jre.12212.

Palmer, L.J., Cooper, P.R., Ling, M.R., Wright, H.J., Huissoon, A. & Chapple I.L.(2012) Hypochlorous acid regulates neutrophil extracellular trap release in humans. *Clinical and Experimental Immunology.* **167**:261-8. doi: 10.1111/j.1365-2249.2011.04518.x.

Roberts, F. A. & Darveau, R.P. (2015) Microbial protection and virulence in periodontal tissue as a function of polymicrobial communities: symbiosis and dysbiosis. *Periodontology 2000*, **69**: 18–27.

Sajic, T., Liu. Y. & Aebersold, R. (2015) Using data-independent, high-resolution mass spectrometry in protein biomarker research: perspectives and clinical applications. *Proteomics Clinical Applications* **9:**307-21. doi: 10.1002/prca.201400117.

Scott, D.A. & Krauss, J. (2012) Neutrophils in periodontal inflammation. *Frontiers in Oral Biology*. **15**:56-83. doi: 10.1159/000329672.

Tonetti, M.S., Eickholz, P., Loos, B.G., Papapanou, P., van der Velden, U., Armitage, G., Bouchard, P., Deinzer, R., Dietrich, T., Hughes, F., Kocher, T., Lang, N.P., Lopez, R., Needleman, I., Newton, T., Nibali, L., Pretzl, B., Ramseier, C., Sanz-Sanchez, I., Schlagenhauf, U. & Suvan, J.E.(2015) Principles in prevention of periodontal diseases: Consensus report of group 1 of the 11th European Workshop on Periodontology on effective prevention of periodontal and peri-implant diseases. *Journal of Clinical Periodontology.* **42** Suppl 16:S5-11. doi: 10.1111/jcpe.12368.

Trindade F., Amado F., Oliveira-Silva R.P., Daniel-da-Silva A.L., Ferreira R., Klein J., Faria-Almeida R., Gomes P.S., Vitorino R. (2015) Toward the definition of a peptidome signature and protease profile in chronic periodontitis. Proteomics Clinical Applications. doi: 10.1002/prca.201400191.

Van Dyke, T.E. (2009) The etiology and pathogenesis of periodontitis revisited. Journal of Applied Oral Science **17**.doi S1678-77572009000100001.

Vizcaíno J.A., Deutsch E.W., Wang R., Csordas A., Reisinger F., Ríos D., Dianes J.A., Sun Z., Farrah T., Bandeira N, Binz PA, Xenarios I, Eisenacher M, Mayer G, Gatto L, Campos A, Chalkley RJ, Kraus HJ,

Albar J.P., Martinez-Bartolomé S., Apweiler R., Omenn G.S., Martens L., Jones A.R., Hermjakob H. (2014). ProteomeXchange provides globally co-ordinated proteomics data submission and dissemination. Nature Biotechnology **30**:223-226. doi:10.1038/nbt.2839

Wiggs, R. & Lobprise, H. (1997) *Veterinary Dentistry, Principles and Practice*. p152. Wiley-Blackwell

Figure legends

Figure 1. Hive panel showing individual hive plots to compare protein levels between very mild gingivitis (G1), moderate gingivitis (G3) and mild periodontitis (PD1) across individuals. All axis show the same magnitude (arbitrary units). Colours denote tooth type (maxilla or mandible): Pink represents tooth 3 incisor; Purple represents tooth 4 canine; Green represents tooth 7 premolar; Turquoise represents tooth 8 premolar; Orange represents tooth 9 molar. The yellow and red boxes highlight samples taken from different teeth but in the same individual animal. Dog ID is shown above or below each plot for reference.

Figure 2. Hive plots comparing average protein levels in all samples between very mild gingivitis (G1), moderate gingivitis (G3) and mild periodontitis (PD1). i. All proteins identified across the experiment, including proteins only identified in one tooth. ii. Proteins identified in all ten teeth; the magnitude of the protein levels found is smaller than for all the proteins and so an enlargement of the core proteins identified in all teeth is also provided.

Figure 3. Hive plots showing ratios of average protein levels between health states in all samples: moderate gingivitis:very mild gingivitis (G3/G1), mild periodontitis:very mild gingivitis (PD1/G1), and mild periodontitis:moderate gingivitis (PD1/G3). i. All proteins identified across the experiment, including proteins only identified in one tooth. ii. Proteins identified in all ten teeth; the magnitude of the fold changes found is smaller than for all the proteins and so an enlargement of the core proteins identified in all teeth is also provided.

Figure 4. Comparison of Haptoglobin quantities determined by ELISA (on left) and mass spectrometry (on right). Data displayed mean +/-SE.

Table 1. Disease scoring system adapted from Marshall et al 2014 to show the stages used in this study. G1: very mild gingivitis; G3: moderate gingivitis; PD1 mild periodontitis

Score	Gingivitis	Periodontal probing depth (mm)	Gingival recession (mm)
G1	Very mild gingivitis (red, swollen but no bleeding on probing)	≥1 to 2	0
G3	Moderate gingivitis (red, swollen and immediate bleeding on probing)	≥1 to 2	0
PD1	Gingivitis must be present (i.e. active periodontitis)	>2 (>3 on canine teeth) to 4 (6 on canine teeth)	>0 to 2 (3 on canine teeth)

Table 2. A summary of the 30 samples used for proteomic discovery. Table shows the unique dog identification number, tooth sampled, age at start of study, gender and the week when the respective sample was taken. G1 represents very mild gingivitis, G3 moderate gingivitis and PD1 mild periodontitis. Teeth are labelled by quadrant (where the first number represents the FDI notation for that quadrant) and position in the quadrant (second and third numbers 03 incisor, 04 canine, 07 premolar, 08 premolar and 09 molar).

Dog ID	Tooth	Sex	Age (years)	Sampling week		
				G1 sample	G3 sample	PD1 sample
MS05164	207	Male	1.3	6	18	42
MS05159	409	Female	1.3	0	24	54
MS04713	104	Male	4.7	0	6	24
MS04713	304	Male	4.7	0	18	24
MS04707	408	Female	4.8	0	18	24
MS04651	208	Female	5.8	0	12	18
MS05027	103	Male	2.4	0	30	42
MS05029	209	Female	2.5	0	6	12
MS05028	108	Male	2.3	18	30	42
MS05028	209	Male	2.3	0	18	42

Table 3. Results of the univariate mixed model analysis comparing each health state, showing the 41 proteins with significant changes at adjusted $p<0.05$. For each health state comparison, the fold change and 95% confidence intervals are shown along with adjusted *p*-values. G1 represents very mild gingivitis, G3 moderate gingivitis and PD1 mild periodontitis.

Accession	**UniProt Annotation**	**Putative Group**	**Putative function**	**PD1/G1 Fold change (CI) & Adjusted *p*-value**	**PD1/G3 Fold change (CI) & Adjusted *p*-value**	**G3/G1 Fold change (CI) & Adjusted *p*-value**
F1PQM1	Purine nucleoside phosphorylase	Biosynthesis	Nucleotide synth - Adenosine to A, Guanosine to G	1.59 (1.12, 2.26) 0.0362	1.55 (1.09, 2.21) 0.0438	1.03 (0.72, 1.46) 1.0000
P19006	Haptoglobin	Blood constituent	Plasma - binds free haemoglobin, inhibits oxidative activity	2.48 (1.32, 4.66) 0.0358	2.42 (1.29, 4.56) 0.0358	1.02 (0.54, 1.92) 1.0000
E2R0T6	Heat shock 70kDa protein 8	House keeping	Multiple including chaperone protein & regulator of apoptosis	1.55 (1.11, 2.16) 0.0364	1.48 (1.06, 2.07) 0.0571	1.05 (0.75, 1.46) 1.0000
E2RAL0	Rho GDP dissociation inhibitor (GDI) beta	House keeping	Cell signalling, proliferation, cytoskeletal organization, and secretion	1.81 (1.16, 2.83) 0.0358	1.87 (1.20, 2.92) 0.0358	0.97 (0.62, 1.51) 1.0000
F1PBZ4	NAD(P)H:quinone oxidoreductase-1	House keeping	Response to oxidative stress	1.68 (1.15, 2.45) 0.0358	1.41 (0.96, 2.05) 0.1732	1.19 (0.82, 1.74) 0.7978
F1PKW7	14-3-3 protein beta/alpha	House keeping	Adapter protein	2.00 (1.32, 3.02) 0.0142	1.75 (1.16, 2.63) 0.0358	1.15 (0.76, 1.73) 0.9630
C0LQL0	S100 calcium binding protein A8	Immunity & inflammation	Subunit of Calprotectin - Putative inflammatory regulator	2.28 (1.30, 3.99) 0.0358	1.55 (0.89, 2.72) 0.2866	1.47 (0.84, 2.57) 0.4270
J9P732	S100 calcium binding	Immunity &	Subunit of Calprotectin - Putative	1.90 (1.17, 3.07)	1.62 (1.00, 2.61)	1.17 (0.73, 1.90)

	protein A9	inflammation	inflammatory regulator	0.0358	0.1124	0.9620
J9PAQ5	S100 calcium binding protein A12	Immunity & inflammation	Putative anti-inflammatory and cell signalling	2.15 (1.24, 3.71) 0.0358	1.84 (1.07, 3.18) 0.0733	1.17 (0.67, 2.02) 1.0000
E2RCI8	Annexin A6	Immunity & inflammation	Structural or anti-inflammatory	1.81 (1.18, 2.78) 0.0358	1.43 (0.93, 2.19) 0.2420	1.27 (0.83, 1.95) 0.6282
F1P6B7	Annexin A1	Immunity & inflammation	Glucocorticoid anti-inflammatory	1.64 (1.22, 2.21) 0.0142	1.36 (1.01, 1.84) 0.0929	1.21 (0.89, 1.62) 0.5154
F1PIC7	Heat shock protein 5 (HSPA5)	Immunity & inflammation	ER overload response	1.74 (1.14, 2.66) 0.0387	1.60 (1.05, 2.45) 0.0738	1.09 (0.71, 1.66) 1.0000
J9NWJ5	Thioredoxin	Immunity & inflammation	Redox signalling and oxidative stress	1.64 (1.15, 2.34) 0.0358	1.56 (1.10, 2.23) 0.0438	1.05 (0.74, 1.50) 1.0000
J9P0R6	Myeloperoxidase	Immunity & inflammation	Neutrophil respiratory burst	1.7 (1.16, 2.51) 0.0358	1.64 (1.11, 2.42) 0.0425	1.04 (0.70, 1.53) 1.0000
J9P969	Neuroblast differentiation-associated protein AHNAK	Immunity & inflammation	Interaction with S100 B protein	1.78 (1.21, 2.62) 0.0329	1.57 (1.07, 2.31) 0.0622	1.13 (0.77, 1.67) 0.9657
P81709	Lysozyme C	Immunity & inflammation	Bacterial peptidoglcyan destruction	1.65 (1.16, 2.35) 0.0358	1.61 (1.13, 2.29) 0.0358	1.03 (0.72, 1.47) 1.0000
Q8MJD1	Neutrophil elastase	Immunity & inflammation	Neutrophil/ macrophages secreted	1.65 (1.13, 2.40) 0.0376	1.59 (1.09, 2.32) 0.0497	1.04 (0.71, 1.51) 1.0000
E2R2C3	Glucose-6-phosphate isomerase	Metabolic	Glycolysis	1.78 (1.36, 2.32) 0.0005	1.61 (1.23, 2.11) 0.0114	1.10 (0.84, 1.44) 0.9393
F1PE09	6-Phosphogluconate	Metabolic	Pentose phosphate pathway	1.63 (1.14, 2.33)	1.54 (1.08, 2.21)	1.05 (0.74, 1.51)

	dehydrogenase			0.0358	0.0521	1.0000
F1PE28	Transketolase	Metabolic	Pentose phosphate pathway	1.86 (1.27, 2.71) 0.0142	1.63 (1.12, 2.38) 0.0387	1.14 (0.78, 1.66) 0.9525
H9GW87	Transaldolase	Metabolic	Links the pentose phosphate pathway to glycolysis	1.67 (1.13, 2.48) 0.0387	1.70 (1.15, 2.51) 0.0358	0.99 (0.67, 1.46) 1.0000
E2QZK2	Uncharacterized protein	NA	Uncharacterized putative gelsolin-like protein	1.62 (1.10, 2.36) 0.0438	1.51 (1.03, 2.21) 0.0816	1.07 (0.73, 1.57) 1.0000
F1PBL1	Uncharacterized protein	NA	Uncharacterized poly(A) RNA binding protein	1.57 (1.09, 2.27) 0.0447	1.51 (1.05, 2.17) 0.0733	1.04 (0.73, 1.50) 1.0000
F1PJ65	Uncharacterized protein	NA	Uncharacterized putative GTPase protein	1.47 (1.06, 2.06) 0.0645	1.54 (1.10, 2.15) 0.0410	0.96 (0.69, 1.34) 1.0000
F1PNY2	Uncharacterized protein	NA	Uncharacterized protein - Ig-like domain	1.97 (1.30, 2.99) 0.0142	1.77 (1.17, 2.68) 0.0358	1.11 (0.73, 1.69) 1.0000
F1PR54	Uncharacterized protein	NA	Uncharacterised transferrin-like protein	1.62 (1.10, 2.39) 0.0465	1.60 (1.08, 2.37) 0.0525	1.01 (0.68, 1.49) 1.0000
J9NYW7	Uncharacterized protein	NA	Uncharacterized protein - Ig-like domain	2.38 (1.33, 4.27) 0.0329	2.08 (1.16, 3.73) 0.0438	1.14 (0.64, 2.05) 1.0000
J9P127	Uncharacterized protein	NA	Uncharacterized poly(A) RNA binding protein	1.57 (1.02, 2.41) 0.0927	1.93 (1.25, 2.97) 0.0301	0.81 (0.53, 1.25) 0.7693
E2QUU4	Keratin, type II cytoskeletal 4	Structural	Cytoskeletal protein	1.86 (1.16, 3.01) 0.0387	1.71 (1.06, 2.76) 0.0733	1.09 (0.68, 1.76) 1.0000
F1PYU9	Keratin, type I cytoskeletal 10	Structural	Cytoskeletal protein	1.51 (1.09, 2.10) 0.0438	1.25 (0.90, 1.73) 0.4321	1.21 (0.87, 1.68) 0.5839
E2R4B0	Keratin 78	Structural	Cytoskeletal protein	1.87 (1.28, 2.73)	1.62 (1.11, 2.37)	1.15 (0.79, 1.68)

				0.0142	0.0425	0.9355
E2R7U2	Keratin 13	Structural	Cytoskeletal protein	1.69 (1.20, 2.38) 0.0301	1.45 (1.03, 2.05) 0.0780	1.16 (0.83, 1.64) 0.8273
E2R8Z5	Keratin 5	Structural	Cytoskeletal protein	1.57 (1.11, 2.23) 0.0405	1.55 (1.09, 2.20) 0.0438	1.01 (0.71, 1.44) 1.0000
E2RB38	Tropomyosin 1	Structural	Actin binding	1.75 (1.17, 2.63) 0.0358	1.66 (1.11, 2.49) 0.0445	1.06 (0.70, 1.58) 1.0000
F1PLS4	Vimentin	Structural	Type III intermediate filament	1.51 (0.99, 2.31) 0.1312	1.78 (1.16, 2.73) 0.0358	0.85 (0.55, 1.29) 0.8977
H9GWE2	Uridine phosphorylase 1	Structural	Interacts with vimentin	1.62 (1.13, 2.32) 0.0358	1.62 (1.13, 2.33) 0.0358	1.00 (0.70, 1.43) 1.0000
E2QWN7	Lymphocyte cytosolic protein 1	Structural	Actin binding	1.83 (1.18, 2.81) 0.0358	1.79 (1.16, 2.76) 0.0358	1.02 (0.66, 1.57) 1.0000
H9GWB1	Histone H2B	Structural	DNA packaging	1.69 (1.17, 2.44) 0.0358	1.43 (0.99, 2.06) 0.1262	1.18 (0.82, 1.70) 0.8201
J9P2B7	Histone H2A	Structural	DNA packaging	1.54 (1.03, 2.31) 0.0816	1.67 (1.12, 2.50) 0.0428	0.92 (0.62, 1.38) 1.0000
L7N0L3	Histone H4	Structural	DNA packaging	1.42 (0.97, 2.09) 0.1644	1.65 (1.12, 2.42) 0.0387	0.86 (0.59, 1.27) 0.9123

Figure 1

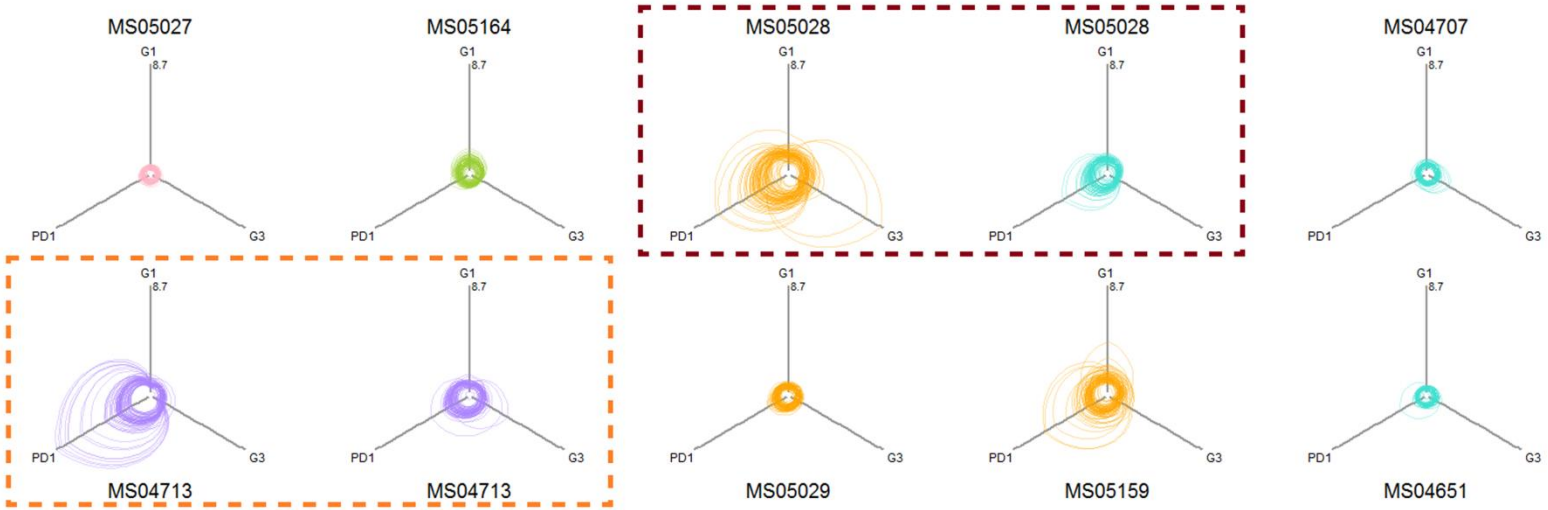
MS05027
MS05164
MS05028
MS05028
MS04707
MS04713
MS04713
MS05029
MS05159
MS04651
G1
8.7
PD1
G3

Figure 2

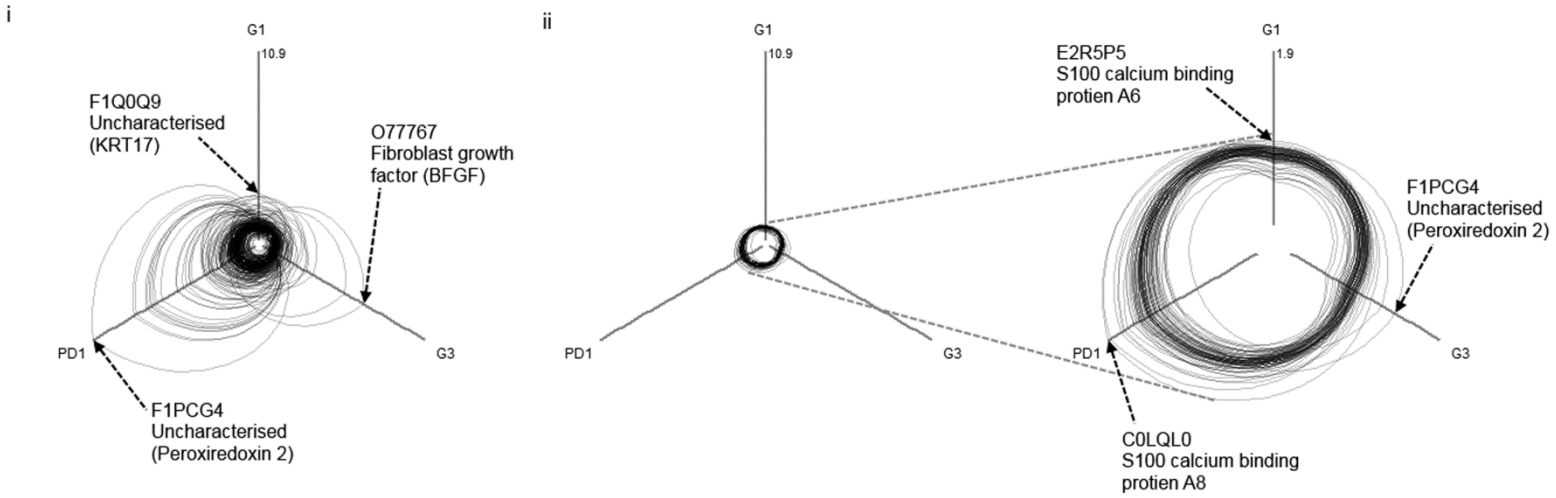
i
G1
10.9
F1Q0Q9
Uncharacterised
(KRT17)
O77767
Fibroblast growth
factor (BFGF)
PD1
G3
F1PCG4
Uncharacterised
(Peroxiredoxin 2)
ii
G1
10.9
G1
1.9
E2R5P5
S100 calcium binding
protien A6
F1PCG4
Uncharacterised
(Peroxiredoxin 2)
PD1
G3
PD1
G3
C0LQL0
S100 calcium binding
protien A8

Figure 3

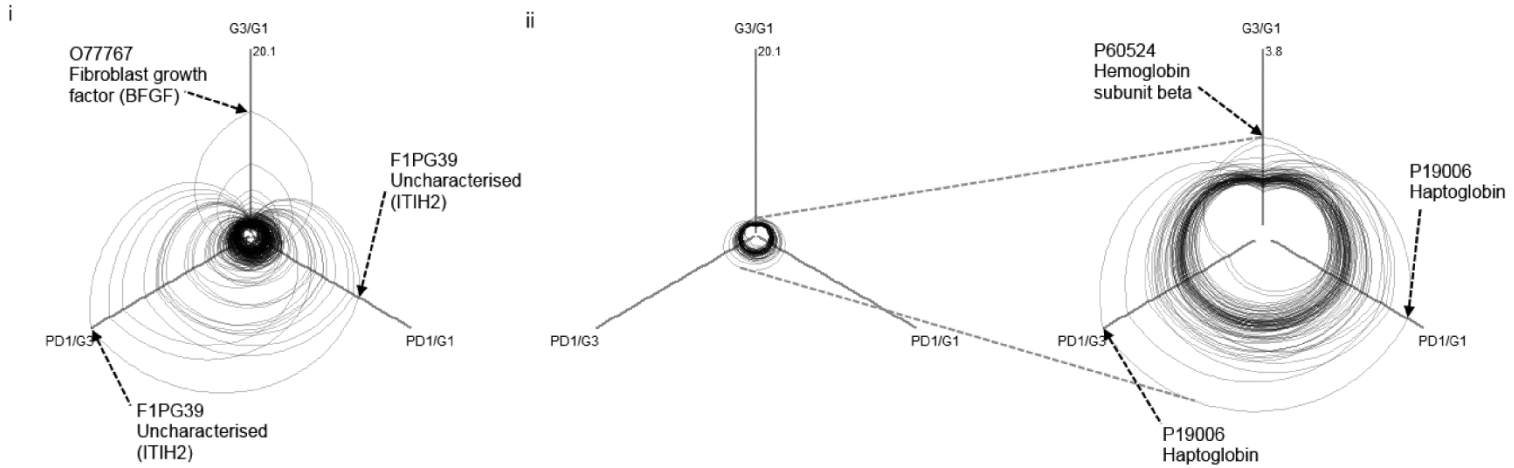
i
G3/G1
20.1
O77767
Fibroblast growth
factor (BFGF)
F1PG39
Uncharacterised
(ITIH2)
PD1/G3
PD1/G1
F1PG39
Uncharacterised
(ITIH2)
ii
G3/G1
20.1
PD1/G3
PD1/G1
G3/G1
3.8
P60524
Hemoglobin
subunit beta
P19006
Haptoglobin
PD1/G3
PD1/G1
P19006
Haptoglobin

Figure 4

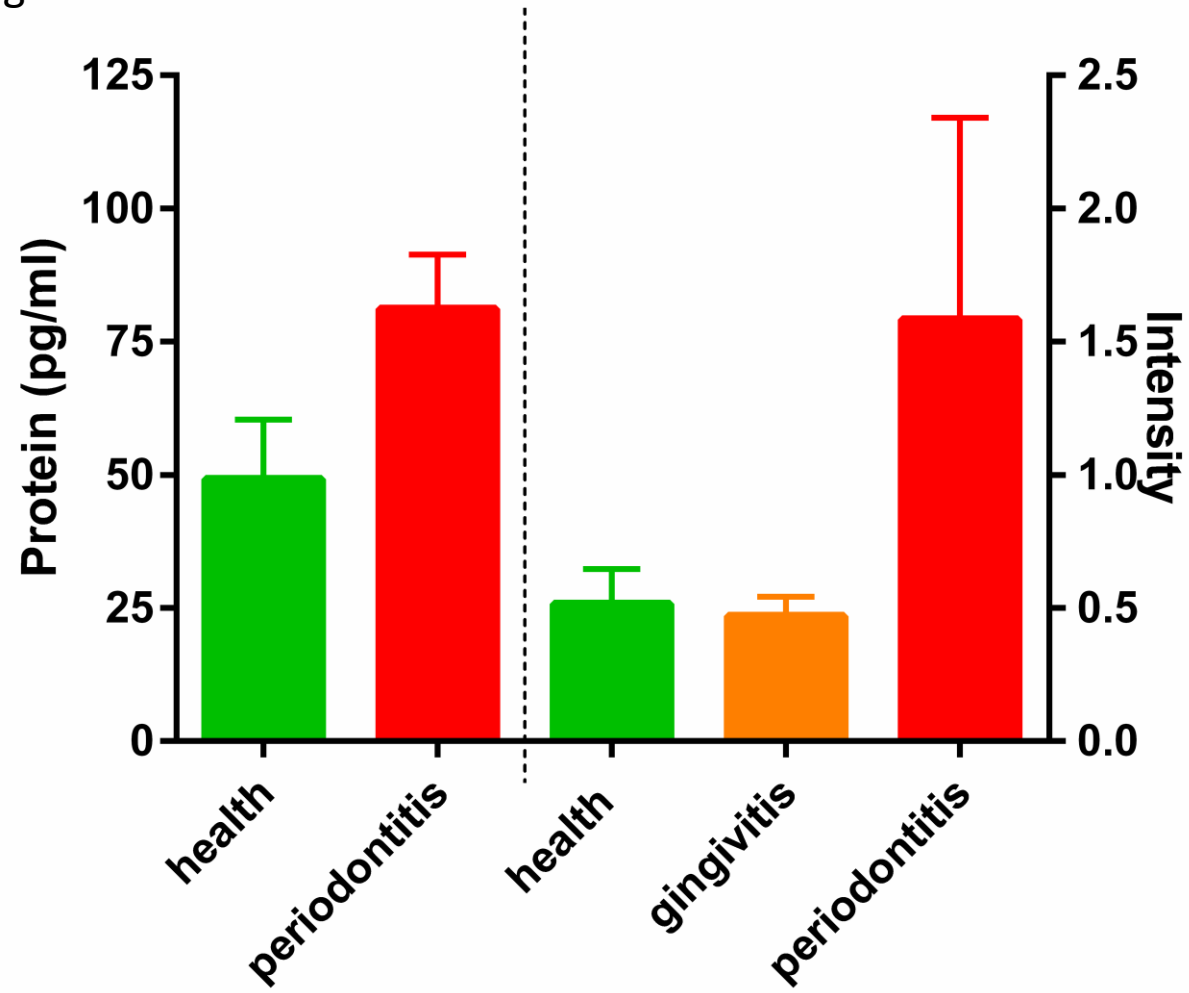
Protein (pg/ml)
125
100
75
50
25
0
Intensity
2.5
2.0
1.5
1.0
0.5
0.0
health
periodontitis
health
gingivitis
periodontitis

Supplemental data

Supplemental Table 1. All proteins identified from GCF with 2 peptides and in all ten teeth. Table shows the listing protein identity (IPI accession number, description and protein identifier), mean coverage, mean number of peptides and PSMs (*peptide spectrum match)* used to identify the protein and the estimated abundance (with 95% CI) of the protein identified in each sample type (relative to the mastermix). G1 represents very mild gingivitis, G3 moderate gingivitis and PD1 mild periodontitis.

Accession	Description	Protein abbreviation	Mean coverage (%)	Mean number of peptides identified	Mean number of PSMs	G1 (95% CI)	G3 (95% CI)	PD1 (95% CI)
A1ILJ0	Alpha 1 antitrypsin		12.7	5	32.5	0.56 (0.29, 1.07)	0.54 (0.28, 1.03)	1.01 (0.53, 1.94)
C0LQL0	S100 calcium binding protein A8	S100A8	58.5	6.6	49.5	0.55 (0.32, 0.97)	0.81 (0.46, 1.42)	1.26 (0.72, 2.21)
D6BR72	Keratin 71	KRT71	19.7	10.6	68.9	0.49 (0.26, 0.95)	0.62 (0.32, 1.2)	0.84 (0.44, 1.63)
E2QUU4	Uncharacterized protein	KRT71	46.4	35.2	248.1	0.56 (0.34, 0.93)	0.61 (0.37, 1.02)	1.04 (0.63, 1.74)
E2QWN7	Uncharacterized protein	LCP1	20.9	11.2	65	0.63 (0.4, 1)	0.64 (0.41, 1.02)	1.15 (0.73, 1.83)
E2QZK2	Uncharacterized protein	GSN	11.2	6.7	30.9	0.7 (0.45, 1.07)	0.75 (0.48, 1.15)	1.12 (0.73, 1.73)
E2QZM1	Uncharacterized protein	YWHAQ	25.3	5.9	45.8	0.75 (0.51, 1.11)	0.74 (0.5, 1.1)	1.09 (0.73, 1.61)
E2R0S6	Annexin	ANXA8L1	21.7	7.4	41.6	0.78 (0.58, 1.05)	0.76 (0.57, 1.03)	0.9 (0.67, 1.22)
E2R0T6	Uncharacterized protein	HSPA8	20.1	12.3	67.4	0.7 (0.48, 1.01)	0.73 (0.51, 1.06)	1.09 (0.75, 1.57)
E2R2C3	Gluce-6-phphate isomerase	GPI	12	5.2	28.3	0.64 (0.46, 0.89)	0.7 (0.5, 0.98)	1.13 (0.81, 1.58)
E2R4	Uncharacterized	CAPG	17.8	5.6	33.6	0.75	0.65	1 (0.71,

13	protein					(0.53, 1.06)	(0.46, 0.92)	1.4)
E2R4B0	Uncharacterized protein	KRT78	14.3	7.7	55.7	0.59 (0.37, 0.94)	0.68 (0.43, 1.09)	1.11 (0.7, 1.76)
E2R5P5	Uncharacterized protein	S100A6	26.7	3.2	14.7	0.84 (0.61, 1.16)	0.76 (0.55, 1.05)	1.05 (0.76, 1.44)
E2R5W6	Uncharacterized protein	GC	16.2	6.7	43.7	0.58 (0.35, 0.98)	0.56 (0.34, 0.95)	0.97 (0.57, 1.63)
E2R662	Uncharacterized protein	TPM4	18.9	6.9	35.1	0.64 (0.42, 0.96)	0.66 (0.44, 1.01)	1.03 (0.68, 1.57)
E2R7A4	Involucrin	IVL	34.9	8.6	53.4	0.76 (0.56, 1.05)	0.78 (0.57, 1.08)	0.96 (0.7, 1.32)
E2R7U2	Uncharacterized protein	KRT13	54	29.4	246.2	0.63 (0.42, 0.94)	0.73 (0.49, 1.09)	1.06 (0.71, 1.58)
E2R8Q7	Uncharacterized protein	KRT15	35.1	19.9	137.4	0.74 (0.5, 1.11)	0.73 (0.49, 1.08)	1.19 (0.8, 1.78)
E2R8Z5	Uncharacterized protein	KRT5	48.5	37.1	299.6	0.65 (0.45, 0.95)	0.66 (0.45, 0.96)	1.02 (0.71, 1.49)
E2RAL0	Uncharacterized protein	ARHGDIB	27.2	3.9	23.3	0.62 (0.39, 1)	0.6 (0.38, 0.97)	1.13 (0.7, 1.81)
E2RB38	Uncharacterized protein	TPM1	22.6	7.3	36	0.66 (0.43, 1.02)	0.7 (0.45, 1.08)	1.16 (0.75, 1.79)
E2RCI8	Annexin (Fragment)	ANXA6	11.1	6.2	27.6	0.61 (0.41, 0.91)	0.78 (0.52, 1.16)	1.11 (0.75, 1.65)
E2RHG2	Uncharacterized protein	PRDX1	31.8	7.4	48.8	0.72 (0.51, 1.02)	0.81 (0.58, 1.15)	1 (0.71, 1.41)
E2RLS3	Uncharacterized protein	SLC29A1	15.2	10.9	63.5	0.74 (0.53, 1.04)	0.72 (0.51, 1.01)	1.1 (0.78, 1.56)
E2RRC9	Phphoglycerate kinase	PGK1	15.3	6.3	24.9	0.75 (0.53, 1.07)	0.7 (0.49, 1)	1.07 (0.75, 1.52)
E2RSI6	Uncharacterized protein	EZR	25.5	17.5	96.9	0.71 (0.5, 1)	0.78 (0.55, 1.1)	1.04 (0.73, 1.48)
F1P6B7	Uncharacterized protein	ANXA1	41.8	14.4	119.3	0.65 (0.48, 0.88)	0.79 (0.58, 1.06)	1.07 (0.79, 1.45)

F1PBL1	Uncharacterized protein	YWHAZ	45.7	9.7	71.3	0.73 (0.52, 1.04)	0.76 (0.54, 1.08)	1.15 (0.81, 1.63)
F1PBZ4	Uncharacterized protein (Fragment)	NQO1	21.6	6.7	58.1	0.66 (0.46, 0.96)	0.79 (0.55, 1.15)	1.12 (0.77, 1.62)
F1PCG4	Uncharacterized protein	PRDX2	18.5	3	18.7	0.46 (0.24, 0.88)	0.68 (0.35, 1.3)	0.72 (0.37, 1.39)
F1PCH3	Enolase	ENO1	33.6	11.9	107.5	0.77 (0.55, 1.09)	0.74 (0.52, 1.05)	0.98 (0.7, 1.39)
F1PCK2	Uncharacterized protein	A1BG	6.3	3.3	15.7	0.59 (0.34, 1.02)	0.51 (0.29, 0.88)	0.93 (0.54, 1.61)
F1PDJ5	Apolipoprotein A-I	APOA1	77.5	29.7	373.9	0.44 (0.23, 0.83)	0.45 (0.24, 0.85)	0.8 (0.43, 1.51)
F1PE09	6-phphogluconate dehydrogenase, decarboxylating	PGD	21.5	10.2	62.6	0.69 (0.49, 0.99)	0.73 (0.51, 1.04)	1.13 (0.79, 1.61)
F1PE28	Uncharacterized protein	TKT	31.6	15.8	72.7	0.65 (0.42, 0.99)	0.74 (0.48, 1.13)	1.21 (0.79, 1.84)
F1PGS2	Fibrinogen beta chain (Fragment)	FGB	9.7	4	15.6	0.47 (0.26, 0.86)	0.52 (0.28, 0.94)	0.99 (0.54, 1.81)
F1PGY1	Uncharacterized protein (Fragment)	HSP90AA1	15.1	9	54.5	0.67 (0.46, 1)	0.74 (0.5, 1.1)	1.08 (0.73, 1.6)
F1PHR2	Pyruvate kinase	PKM	26.9	12.5	84.9	0.67 (0.48, 0.92)	0.7 (0.51, 0.97)	1.05 (0.76, 1.45)
F1PIC7	Uncharacterized protein	HSPA5	8.9	4.8	26.1	0.65 (0.41, 1.02)	0.7 (0.45, 1.11)	1.13 (0.71, 1.78)
F1PJ65	Uncharacterized protein	IQGAP1	4.7	5.1	23.5	0.76 (0.55, 1.05)	0.73 (0.53, 1.01)	1.12 (0.81, 1.55)
F1PKW7	Uncharacterized protein	YWHAB	25.7	5.9	44.8	0.61 (0.4, 0.93)	0.7 (0.46, 1.06)	1.22 (0.81, 1.85)
F1PL93	Uncharacterized protein	ARHGDIA	19.1	3.3	20.3	0.72 (0.5, 1.04)	0.69 (0.48, 0.99)	1.06 (0.74, 1.53)
F1PLS4	Uncharacterized protein	VIM	17.1	9	43	0.74 (0.48, 1.13)	0.62 (0.41, 0.95)	1.11 (0.73, 1.7)
F1PNY2	Uncharacterized protein		8.8	2	9.9	0.54 (0.32,	0.6 (0.35,	1.07 (0.62,

						0.93)	1.03)	1.83)
F1PQ93	Uncharacterized protein	SFN	47.6	10.5	72.5	0.77 (0.55, 1.06)	0.73 (0.53, 1.01)	0.97 (0.7, 1.34)
F1PQM1	Purine nucleide phphorylase	PNP	25	6.2	41	0.73 (0.52, 1.02)	0.74 (0.53, 1.04)	1.16 (0.82, 1.62)
F1PQN5	Uncharacterized protein (Fragment)	CFL1	33.9	4.9	26.4	0.79 (0.55, 1.14)	0.69 (0.48, 1)	1.07 (0.74, 1.54)
F1PR54	Uncharacterized protein	LTF	17.8	11.6	61.1	0.67 (0.45, 1)	0.68 (0.45, 1.01)	1.09 (0.73, 1.62)
F1PSX2	Uncharacterized protein (Fragment)		50.3	3.6	52.6	0.52 (0.28, 0.95)	0.63 (0.35, 1.16)	0.98 (0.54, 1.79)
F1PTS8	Uncharacterized protein (Fragment)	KRT6A	43	29.8	224.9	0.75 (0.51, 1.1)	0.79 (0.54, 1.16)	0.98 (0.67, 1.45)
F1PVW0	L-lactate dehydrogenase	LDHA	31.7	10.5	63.4	0.78 (0.56, 1.1)	0.77 (0.55, 1.08)	1.13 (0.8, 1.59)
F1PYE3	Heat shock protein beta-1	HSPB1	34.4	8.1	62	0.75 (0.54, 1.04)	0.76 (0.55, 1.06)	0.87 (0.62, 1.21)
F1PYU9	Keratin, type I cytkeletal 10	KRT10	26.5	16.1	103.8	0.67 (0.44, 1.03)	0.81 (0.53, 1.25)	1.01 (0.66, 1.56)
F1PZR4	Uncharacterized protein	HPX	10.6	4.1	25.5	0.41 (0.23, 0.75)	0.41 (0.23, 0.75)	0.81 (0.44, 1.46)
F1Q0R0	Uncharacterized protein	KRT16	36.9	20.3	156.3	0.67 (0.46, 0.99)	0.66 (0.45, 0.97)	0.98 (0.67, 1.44)
F1Q3U2	Uncharacterized protein	KRT76	28.8	24.1	143.4	0.55 (0.32, 0.96)	0.55 (0.31, 0.96)	1.03 (0.59, 1.79)
G1K267	Uncharacterized protein		9.9	5.9	29.1	0.66 (0.46, 0.96)	0.67 (0.46, 0.97)	0.89 (0.62, 1.3)
H9GW87	Transaldolase	TALDO1	19	7.7	33.4	0.7 (0.48, 1.02)	0.69 (0.47, 1.01)	1.17 (0.8, 1.71)
H9GWB1	Histone H2B	LOC478743	38.1	5.7	53.1	0.64 (0.4, 1.03)	0.76 (0.47, 1.22)	1.09 (0.68, 1.74)
H9GWE2	Uncharacterized protein	UPP1	11.5	2.9	15.7	0.68 (0.47, 0.99)	0.68 (0.47, 0.99)	1.11 (0.76, 1.6)
J9NW	Thioredoxin	TXN	25.7	3.2	16.9	0.68	0.72	1.12

J5	(Fragment)					(0.46, 1)	(0.49, 1.05)	(0.76, 1.64)
J9NYW7	Uncharacterized protein (Fragment)		13.3	5.9	69.8	0.44 (0.24, 0.79)	0.5 (0.28, 0.91)	1.05 (0.58, 1.89)
J9P0R6	Uncharacterized protein	MPO	14.5	9.8	64.2	0.65 (0.43, 1)	0.68 (0.45, 1.03)	1.12 (0.73, 1.7)
J9P127	Uncharacterized protein	LOC100683370	55.2	5.3	29.7	0.7 (0.46, 1.07)	0.57 (0.37, 0.87)	1.09 (0.71, 1.68)
J9P2B7	Histone H2A	LOC488299	31	4	35.5	0.72 (0.48, 1.1)	0.67 (0.44, 1.01)	1.12 (0.74, 1.69)
J9P4Y2	Uncharacterized protein	S100A2	32.6	5.2	39.5	0.7 (0.51, 0.97)	0.87 (0.63, 1.19)	1.09 (0.79, 1.49)
J9P732	Uncharacterized protein (Fragment)	S100A9	25	8.3	43.9	0.65 (0.42, 1)	0.76 (0.49, 1.18)	1.23 (0.79, 1.91)
J9P969	Uncharacterized protein	AHNAK	15.8	12.7	66.6	0.62 (0.41, 0.94)	0.7 (0.46, 1.07)	1.1 (0.72, 1.67)
J9P9J6	Uncharacterized protein		12.8	4.5	36.1	0.35 (0.19, 0.67)	0.44 (0.23, 0.84)	0.63 (0.33, 1.19)
J9PAQ5	Uncharacterized protein	S100A12	64	10	101.6	0.54 (0.3, 0.95)	0.62 (0.35, 1.1)	1.15 (0.65, 2.03)
J9PBN6	Uncharacterized protein	LOC611458	6.4	9.5	37.4	0.44 (0.24, 0.79)	0.43 (0.24, 0.78)	0.86 (0.47, 1.55)
L7N094	Uncharacterized protein	KRT3	23.6	21.4	172	0.64 (0.4, 1.04)	0.7 (0.43, 1.12)	1.08 (0.67, 1.74)
L7N095	Uncharacterized protein (Fragment)	KRT5	45.4	30.6	236.7	0.65 (0.44, 0.98)	0.68 (0.45, 1.02)	0.98 (0.65, 1.48)
L7N0F2	Uncharacterized protein	LOC486474	42.3	3.6	50.7	0.45 (0.24, 0.84)	0.51 (0.27, 0.97)	0.87 (0.46, 1.63)
L7N0L3	Histone H4 (Fragment)	LOC611192	58.3	7.7	77.3	0.74 (0.48, 1.15)	0.64 (0.41, 1)	1.05 (0.68, 1.64)
P05124	Creatine kinase B-type	CKB	15.4	4.5	29	0.79 (0.54, 1.15)	0.78 (0.54, 1.14)	0.93 (0.64, 1.35)
P19006	Haptoglobin	HP	29.3	9.9	66.4	0.37 (0.21, 0.66)	0.38 (0.21, 0.67)	0.91 (0.51, 1.62)

P49822	Serum albumin	ALB	62.6	45.4	536.3	0.62 (0.32, 1.2)	0.64 (0.33, 1.25)	0.88 (0.45, 1.72)
P54714	Triephphate isomerase	TPI1	31.1	6.3	30.9	0.72 (0.52, 1.01)	0.71 (0.51, 0.99)	1.04 (0.74, 1.46)
P60524	Hemoglobin subunit beta	HBB	86.3	16.4	322.7	0.18 (0.06, 0.51)	0.24 (0.09, 0.68)	0.39 (0.14, 1.1)
P81709	Lysozyme C, spleen isozyme		34.3	4.9	25.2	0.58 (0.37, 0.92)	0.6 (0.38, 0.95)	0.96 (0.61, 1.53)
Q6TEQ7	Annexin A2	ANXA2	41.2	16.1	106.5	0.76 (0.54, 1.07)	0.77 (0.55, 1.09)	1.07 (0.77, 1.51)
Q8MJD1	Neutrophil elastase	ELA2	12.6	3.4	14.4	0.69 (0.46, 1.02)	0.71 (0.48, 1.06)	1.13 (0.76, 1.68)
Q9MZD3	Peptidyl-prolyl cis-trans isomerase (Fragment)		29.3	5.7	40.1	0.61 (0.33, 1.11)	0.55 (0.3, 1.01)	1 (0.55, 1.83)

Supplemental Table 2. Data from ELISAs for haptoglobin, S100A8, myosin 9, keratin type 1 cytoskeletal 10, pyruvate kinase and anti-immunoglobulin binding protein (IBPAb). Those marked in red are below lower limit of detection. G1 represents very mild gingivitis and PD1 mild periodontitis.

Dog Name	Dog ID	Tooth	Haptoglobin (ng/ml)	
			G1 State	PD1 State
Dickens	MS04594	108	11.45	33.01
Dallas	MS04595	208	31.68	116.46
Winston	MS04648	408	>131.15	>131.15
Emerald	MS04650	108	89.63	86.90
Nettie	MS04923	208	81.52	121.03
Eddie	MS04714	208	42.89	102.00
Edna	MS04715	308	98.04	64.93
Whoopee	MS05108	308	3.70	85.47
Bramble	MS05151	109	41.94	41.94
Yoshi	MS05118	308	41.92	78.38

Dog Name	Dog ID	Tooth	S100A8 (pg/ml)	
			G1 State	PD1 State
Dallas	MS04595	209	848.50	162.17
Edna	MS04715	309	350.55	197.55
Jigsaw	MS04846	209	149.47	228.30
Nettie	MS04923	409	101.26	354.26
Noodle	MS04924	408	112.21	151.05

Vinnie	MS05028	409	174.11	324.80
Valerie	MS05030	308	104.51	660.86
Whoopee	MS05108	309	191.41	623.69
Winston	MS04648	109	463.30	325.65
Oxo	MS04935	308	431.53	206.58

Dog Name	Dog ID	Tooth	Myosin 9 (pg/ml)	
			G1State	PD1 State
Dallas	MS04595	308	19.68	32.30
Rooney	MS04599	408	25.49	32.68
Mimi	MS04645	309	22.90	24.92
Winston	MS04648	208	32.58	33.84
Eddie	MS04714	207	27.67	32.43
Emerald	MS04650	308	33.50	30.59
Jigsaw	MS04846	308	40.43	24.93
Ethel	MS04707	308	34.80	30.17
Nettie	MS04923	309	17.98	29.88
Custard	MS05159	209	50.50	30.12

Dog Name	Dog ID	Tooth	Keratin type 1 cytoskeletal 10 (ng/ml)	
			G1State	PD1 State
Winston	MS04648	308	0.83	0.57
China	MS04563	109	0.11	0.63
Bramble	MS05151	409	0.43	0.32
Mimi	MS04645	308	0.19	0.36
Arnie	MS04561	408	<0	0.16
Colin	MS05164	104	0.18	0.41
Chesney	MS05163	408	<0	0.46
Brock	MS05156	208	0.41	0.73
Bentley	MS05152	309	0.46	0.41
Wanda	MS05113	204	0.45	0.45

Dog Name	Dog ID	Tooth	Pyruvate Kinase (ng/ml)	
			G1State	PD1 State
Nettie	MS04923	308	0.55	0.48
Vinnie	MS05028	309	0.03	0.25
Violet	MS05031	309	0.35	0.50
Whoopee	MS05108	409	0.76	0.17
Wotsit	MS05112	308	0.21	0.45

Bramble	MS05151	308	0.07	0.15
Yetti	MS05120	209	1.15	0.41
Yoda	MS05119	309	0.41	1.07
Yasmine	MS05114	408	0.44	0.40
Yoshi	MS05118	309	0.40	0.57

Dog Name	Dog ID	Tooth	IBPAb (ug/ml)	
			G1State	PD1 State
Edna	MS04715	409	<0.07812	<0.07812
Jigsaw	MS04846	409	<0.07813	<0.07812
Nettie	MS04923	209	0.1911	<0.07812
Noodle	MS04924	409	<0.07813	<0.07812
Niamh	MS04930	308	0.3394	<0.07812
Oxo	MS04935	408	0.2404	<0.07812
Usher	MS05024	209	0.3755	<0.07812
Vinnie	MS05028	208	<0.07812	<0.07812
Valerie	MS05030	408	<0.07812	<0.07812
Bramble	MS05151	204	<0.07812	<0.07812